A NOVEL MPPT TECHNIQUE USING IWO METHOD FOR PV GENERATION UNDER PARTIAL SHADING CONDITION

Dr. Madisa
V G Varaprasad Assistant Professor, Electrical and Electronics Engineering,
Vignan's Institute of Information Technology,
Besides Vsez, Duvvada, Vadlapudi, Gajuwaka,
Visakhapatnam, Andhra Pradesh 530049

K.Anusha
Electrical and Electronics Engineering
Vignan's Institute of Information Technology
Besides Vsez, Duvvada, Vadlapudi, Gajuwaka,
Visakhapatnam, Andhra Pradesh 530049

A.Nancy Hanna
Electrical And Electronics Engineering,
Vignan's Institute of Information Technology,
Besides Vsez, Duvvada, Vadlapudi, Gajuwaka,
Visakhapatnam, Andhra Pradesh 530049

G. Revathi
Electrical and Electronics Engineering,
Vignan's Institute of Information Technology,
Besides Vsez, Duvvada, Vadlapudi, Gajuwaka,
Visakhapatnam, Andhra Pradesh 530049

M.Sunil
Electrical and Electronics Engineering,
Vignan's Institute of Information Technology,
Besides Vsez, Duvvada, Vadlapudi, Gajuwaka,
Visakhapatnam, Andhra Pradesh 530049

Abstract: **A Modified Invasive Weed Optimization (MIWO) technique is developed and integrated using perturb & observes (P&O) algorithm to extract the maximum power from photovoltaic (PV) system under rapid climate changes as well as partial shading condition. Extracting the maximum power from PV under partial shading condition is challenging because of conventional P&O algorithm fails to extract the maximum power point (MPP) under partial shaded condition because of its many maximum power points. In such conditions, evolutionary optimization techniques can achieve global maximum power point. The proposed MIWO based P&O algorithm updates reference voltage to operate the PV system at MPP according to weather conditions. DC-DC Boost converter is employed to extract the maximum power from PV system and feed to dc-loads. Rapid weather changes are considered for case studies. MATLAB results through OPAL-RT platform by using Hardwre-in-Loop (HIL) are presented to validate the performance of the proposed method. Small signal analysis also reported in this paper for better analysis. The robustness design of the loop is also studied. For a given set of system parameters, simulations for the small signal model and robustness studies are also carried out to verify the results.**

Keywords: Photovoltaic (PV), Invasive Weed Optimization, Perturb and Observe, Small signal analysis, HIL, OPAL-RT

I. INTRODUCTION

More than two centuries of past industrialization exploited non-renewable energy resources, however, often with undesirable side effects such as pollution and other damage to the natural environment [1]. **S**olar photovoltaic (PV) is anticipated to be a popular source of renewable energy due to

several advantages, notably low operational cost, almost maintenance free and environmentally friendly. Photovoltaic energy is the most important renewable energy resource since it is clean, pollution free, and inexhaustible. The most relevant goals of PV energy include a 40 % cost reduction of PV panels and of the power-converter stage within five years, increased in efficiency of both panels and converters [2-3], and considerable improvement in converter reliability [4]. The rapid growth in the semiconductor and power electronics methods makes PV energy is of increasing demand in electrical power applications. It is important to operate PV energy conversion systems near the maximum power point to increase the output power of PV arrays [5-6]. Inspite of the high cost of solar modules, PV power generation systems, in particular the grid-connected type, have been commercialized in many countries because of its long-term benefits [7-13].

The PV based stand-alone system is widely used in remote places where electricity access is not viable. The stand-alone configuration can provide a well-regulated load voltage, but the continuity of power supply cannot be guaranteed [14]. Output power of PV system is not always constant because of undesirable weather conditions. Hence battery needs to be integrated for flexible operation. Therefore, storage batteries are widely used to improve the continuity of supply in the stand-alone system [14]. In addition to that, power electronics are an integral part of these stand-alone systems as they convert generated electricity into utility-compatible forms. However, the addition of power electronics results in increasing in costs as well as certain reliability issues [15].

Indeed an effective solution must ensure that the PV generator runs at the maximum power point (MPP), then the system can operate at a high efficiency level [1, 4-11, 13-17]. It can be achieved by using maximum power point tracker (MPPT) converter along with suitable algorithm. MPPT is important in PV systems because it reduces the cost of the array by decreasing the number of solar panels needed to generate the desired output power [16]. In general, a PV source is operated in addition with a dc–dc power converter, whose duty ratio is modulated in order to track the instantaneous MPP of the PV source. Several tracking schemes have been proposed by many researchers [1, 4-11, 13-17]. Among them, the popular tracking techniques are perturb and observe (P&O) , hill climbing [18], incremental conductance, short circuit current, open-circuit voltage, and ripple correlation approaches. Some modified techniques have also been suggested, with the objective of minimizing the hardware or improving the performance of the system [19].

The low complexity and low implementation cost make the P&O technique more widely used in commercial products for MPPT [18]. The voltage-based P&O technique is widely used because of its inherent stability with respect to the irradiance variation due to the logarithmic dependence of the PV voltage with respect to the solar irradiance level [20].

The tracking schemes aforementioned are effective under uniform solar irradiation (G), where the P–V curve of a PV module display only one MPP for a given temperature and irradiation. However, a major disadvantages of the PV source is its ineffectiveness during the nights ,low solar irradiance periods, during partially shaded conditions. High initial capital cost has been another deterrent in the popularity of PV systems [19]. Shadowing effects are general phenomena and it mainly causes by clouds and bodies surrounding the plant, manufacturing tolerances, non-uniformity of ambient temperature in proximity of each module due to uneven sun irradiation and air circulation, dust and spot dirtiness such as leaves or bird droppings, PV cell or PV glass protection damages, etc. [21].

The characteristics get more difficult if the entire array does not receive uniform solar irradiance, as in partially shaded conditions, resulting in multiple power peaks. The presence of multiple peaks reduces the effectiveness of the existing MPPT schemes due to their inability to discriminate between the local and global peaks [10, 13, 19, 22-24]. Rapidly changing shadow conditions increase the complexity of MPPT. It is very hard to identify the global maximum power point (GMPP) because multiple local MPPs exist, and their locations fluctuate rapidly corresponding to the changing shading conditions [23].

The presence of multiple peaks reduces the effectiveness of the existing MPPT schemes, which assume a single peak power point on the P–V characteristic. The occurrence of partially shaded conditions being quite common, there is a need to develop special MPPT schemes that can track the global peak under these conditions [13, 19].

MPPT can be achieved by regulating PV voltage at voltage corresponding to the maximum power point (V_{mpp}) [16]. However, the conventional P&O algorithm fails to take the proper V_{mpp} under partial shading of PV system due to its having many local maximum points of power. Therefore, the global maximum point needs to be found out and it is possible by using evolutionary optimization techniques [13, 25]. To find out the proper global maximum point, P&O algorithm is integrated with an optimization technique. A good solution can get by using optimization technique, this good solution may lead to great benefit such as saving weight or improve performance [26]. An Invasive Weed Optimization (IWO) is inspired from colonizing weeds, which has better robustness, adaptation and randomness similar to colonizing weeds [26]. IWO is a population based search technique and widely used in application of engineering due to the following properties [26-27].

1. IWO may create new weeds from any existing weed. Weeds with the highest fitness value can create more weeds, whereas weeds with the lowest fitness value can develop less weeds around their parent weed. As a result, this characteristic promotes IWO convergence.
2. The new weeds are evenly scattered over the search area. Because the normal distribution generates random numbers without mating, no two weeds can be in the same place at the same time. IWO searches the entire search space because of this attribute.

Due to the above mentioned features, IWO can effectively search GMPP of a PV under partial shading condition. Hence, integration of P&O with IWO can give effective solution. In this paper, a simple PV system feed of dc-loads through boost converter along with a modified IWO (MIWO) integrated with P&O algorithm is considered as shown in Fig. 1.

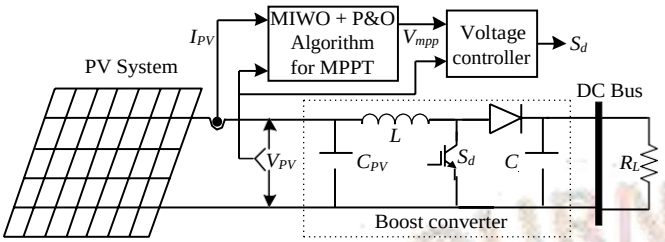

Fig. 1: PV system with boost converter for MPPT

II. PV SYSTEM

The PV system with shading pattern is modeled in MATLAB from [22, 23]. A PV array can be considered a voltage-controlled current source connected across diode [24]. The PV cell diagram is shown in Fig. 2. The PV array is described by current-voltage characteristic function [16] as:

$$I_{PV} = n_p I_{ph} - I_{rs}\left[\exp\left(\frac{q(V_{PV} + I_{PV}R_s)}{AKTn_s}\right) - 1\right] - \frac{V_{PV} + I_{PV}R_s}{R_{sh}} \quad (1)$$

where n_s and n_p are the number of cells connected in series and in parallel, q=1.602·10^{-19} , C is the electron charge, K=1.3806·10^{-23} J/K is Boltzman's constant, A=2 is the p-n junction's ideality factor, T is the cell's temperature (K), I_{ph} is the cell's photocurrent (it depends on the solar irradiation and temperature), $I_{ph} = Isc\frac{G}{G^*}$, I_{rs} is the cell's reverse saturation current, G is the solar irradiance and V_{PV} is cell voltage.

According to P-V characteristics of PV system, PV can generate maximum power at particular voltage which is called as the voltage at maximum power point (V_{mpp}). The P-V characteristics with different levels of irradiance are shown in Fig. 3 under consideration of uniform irradiance.

$$I = I_d - I_{rs}\left[\exp\left(\frac{q(V_{PV} + I_{PV}R_S)}{AKTn_S}\right) - 1\right] \quad \ldots\ldots\ldots\ldots (2)$$

Where I_d represents current flowing through the diode in Fig. 2.

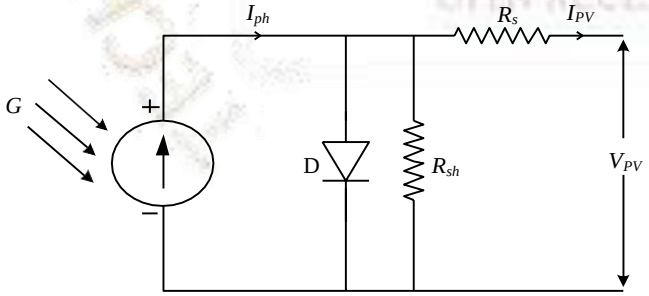

Fig. 2: PV cell

III. MPPT SYSTEM

a) P&O algorithm

The P&O algorithm has the advantage of simple software and hardware realization [18]. In this implementation, the reference voltage (V_{mpp}) is perturbed in an arbitrary direction and the power levels of two consecutive samples are compared. Depending upon the sign of the power change, the direction for further perturbation is decided. A feedback control loop ensures that the output voltage tracks its reference. The following equation is followed to locate the voltage at which the MPP is reached [16, 18].

$$V_{mpp}(k) = V_{mpp}(k-1) + \Delta V \times \text{sign}\left(\frac{dP_{PV}}{dV_{PV}}\right) \quad (3)$$

where, ΔV is steep voltage and k is the iteration.

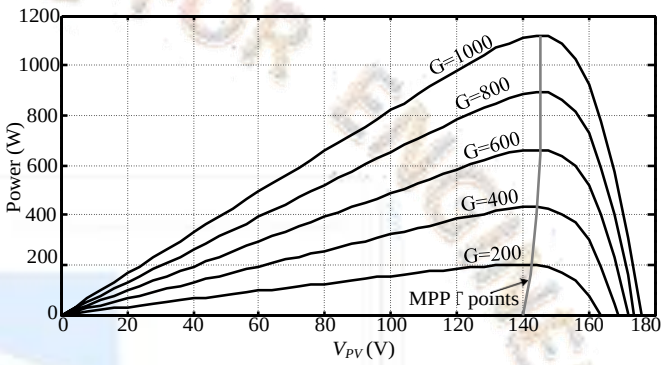

Fig. 3: P-V characteristics under different solar irradiances

However, because of several local maximum power points, the traditional P&O algorithm fails to track proper point under partial shadowed conditions, as illustrated in Fig. 4. As a result, the MIWO technique is combined with the P&O algorithm to track the global maximum point across all maximum power points.

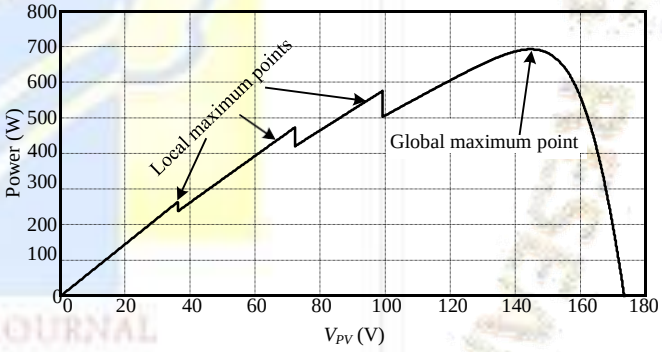

Fig. 4: P-V characteristics under partial shading condition

Because of its simplicity, low cost, and great efficiency, the boost converter, also known as the step-up converter, is regarded the most favourable dc–dc converter architecture in this application [28]. As a result, boost converters are used in this paper for MPPT converters, as illustrated in Fig. 1. For effective system operation under varied conditions, a modified IWO (MIWO) algorithm was implemented.

B) IWO algorithm

Mehrabian and Lucas presented invasive weed optimization in 2006 [29], which is a population-based stochastic optimization technique based on the behaviour of weed colonisation. It has piqued the researcher's interest for over a decade. It has been used in many Engineering and Science applications due to its superior qualities such as reproduction, spatial dispersal, and competitive exclusion when compared to other state-of-the-art evolutionary algorithms. IWO entails the following phases in general.

Step-1: *Initialization:* A finite number of a population is generated randomly over the search space within the variables scope.

Step-2: *Reproduction:* After getting into a blooming tree, each candidate weed of the population is allowed to produce new weeds and the number of new weeds of a candidate weed depends on its relative best and worst fitness value. It is linearly decreased from an allowable maximum weed () to minimum weeds (S_{mim}) with $S_{\max}$ for the best candidate weed, S_{mim} for the worst candidate weed in the population.

$$n(w_i) = \frac{S_{\max}(\max\ fit - fit(w_i)) + S_{\min}(fit(w_i) - \min\ fit)}{\max\ fit - \min\ fit} \quad (4)$$

where $n(w_i)$ = the number of producing seeds of i^{th} weed, $S_{\max}$ and $S_{\min}$ are predefined parameters. $fit(w_i)$ is the fitness value of i^{th} weed, max *fit* and min *fit* are maximum and minimum fitness values of the population respectively.

Step-3: *Spatial dispersal:* The new generated weeds are normally distributed over the search space with mean of parent weed position and the varying standard deviation, defined as

$$\sigma_{gen} = \frac{(gen_{\max} - gen)^{mi}}{gen_{\max}^{mi}}(\sigma_{\max} - \sigma_{\min}) + \sigma_{\min} \quad (5)$$

where σ_{gen} is the standard deviation (SD) at the present generation, $\sigma_{\max}$ and $\sigma_{\min}$ are the maximum and minimum standard deviations, predefined parameters, $gen_{\max}$ is the maximum generations, *mi* is the nonlinear modulation index and necessity of *mi* is generated seeds could be close to the parent weed.

Step-4: *Competitive Exclusion:* If a plant leaves no offspring, then it would go extinct, otherwise they would take over the world. Sources will be for some weeds in the field, as there is a competition between weeds to limit the number of weeds in the population. If the sum of parent weeds and the new generated weeds exceeds the maximum limit ($W_{\max}$), the weeds having worst fitness value are removed up to $W_{\max}$ from the population.

Step-5: *Termination Condition:*

1) The present iteration is equal to the upper limit of number of iterations

2) The above process (Steps 1-4) has been reached the maximum number of fitness evaluations

3) $|f(x^*) - f(x)| \le \varepsilon$ where x^* is the best known optimal solution, x is the best solution obtained by the present method and ε is a small tolerance value, is defined by the user. If the process (Steps 1-4) meets any one of the aforementioned conditions, it will be stopped.

Generally Gaussian function is used in IWO algorithm. For IWO algorithm reproduction mode, it can generate offspring based on the parent individual super posited Gauss distribution of random variables. In order to find the optimal reproductive performance, Cauchy distribution function can give better results instead of Gauss distribution [26, 30]. According to definitions, the Cauchy and Gauss probability density functions are shown in Fig. 5 [26, 30].

From Fig. 5, the Cauchy distribution is smaller than Gauss distribution in vertical direction. Moreover, in horizontal direction, Cauchy distribution has become wider when it is near the horizontal axis. Therefore, the Gaussian distribution function has a greater probability to generate small perturbations, but not very large disturbance [26]. But the Cauchy distribution function has small perturbations capacity than Gauss function, but it is stronger than Gauss in large distribution. Further, it is clear from Fig. 5, the Cauchy distribution is more likely to generate an offspring further away from its parent than a Gaussian distribution due to its long flat tails [30]. It is expected to have a higher probability of escaping from a local optimum or moving away from a plateau, especially when the "basin of attraction" of the local optimum or the plateau is large relative to the mean steep size [30]. Therefore, the character of Cauchy distribution can better maintain the population diversity and make the algorithm a better global optimization algorithm and reliability. Hence, the Cauchy distribution function can get rapidly, optimal solution [26, 30]. Therefore, the Cauchy distribution function is used in IWO algorithm instead of Gaussian distribution function and it is called as modified IWO (MIWO) algorithm. Generally, weather conditions will rapidly change, hence, in this paper implemented MIWO algorithm.

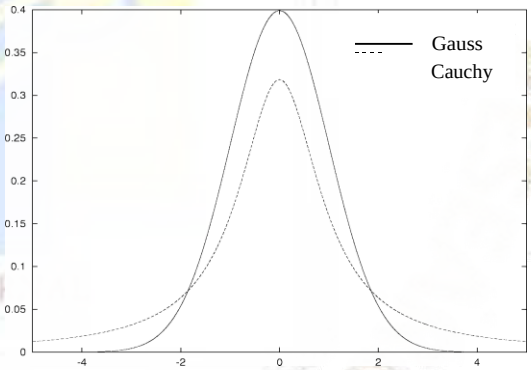

Fig. 5: Cauchy and Gauss distribution probability density function [26, 30]

The one dimensional Cauchy density function centered at the origin is defined by [30]

$$f(x) = \frac{1}{\pi}\frac{t}{t^2 + x^2}, \qquad -\infty < x < \infty \quad (6)$$

where t > 0 is a scale parameter. The corresponding distribution function [30] is

$$F(x) = \frac{1}{2} + \frac{1}{\pi}\arctan\left(\frac{x}{t}\right) \quad (7)$$

In MIWO, $W_{\max}$ seeds are generated around the parent seed. The same principle is applied here and generated $W_{\max}$

voltage points around previous voltage value. Further, P&O algorithm is also included to generate new value of voltage. Hence, **Error! Bookmark not defined.**number of new calculated PV cuthe number can get from W_{max} number of voltages. Therefore W_{max} number of power points can calculate.d finally optimized P_{PV}^{max}. This process will be continued up to completion of search space. The new value of voltage can be obtained by

$$V_{new}^{i} = V_{old}^{i} + m\sigma_{gen}\delta_i, \quad i = 1, ..., W_{max} \tag{8}$$

where, δ_i is a standard Cauchy random variable and

$$m = \Delta V \times \text{sign}\left(\frac{dP_{PV}^{max}}{dV_{mpp}}\right)$$

C) Boost converter

Figure 6 depicts the circuit with a controller that will be used for the boost converter for MPPT of PV system. The control signal (i.e., duty cycle (D)) contains pulses with constant width in steady state. The switch (S_d) is ON during t_{on} and OFF during t_{off}. The voltage across the inductor (V_L) is equal to the input voltage, V_{PV}, during t_{on}. The inductor current, I_L is proportional to the integral of V_L. In this paper boost converter is a modelled form [31, 32]. Reference dc-voltage (input voltage) of boost converter is obtained from integration of MIWO with P&O algorithm. This signal is compared with actual input voltage and error is given to proportional plus integral (PI) controlling. The PI controller can generate duty cycle for S_d. In this paper, ITSE [33] method is used for tuning the gains of PI controller. The boost converter controller is called as a dc-link voltage controller as shown in Fig. 1. The flowchart of the proposed system is shown in Fig. 7.

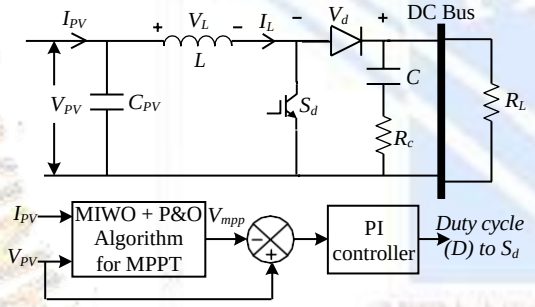

Fig. 6: Boost converter with controller

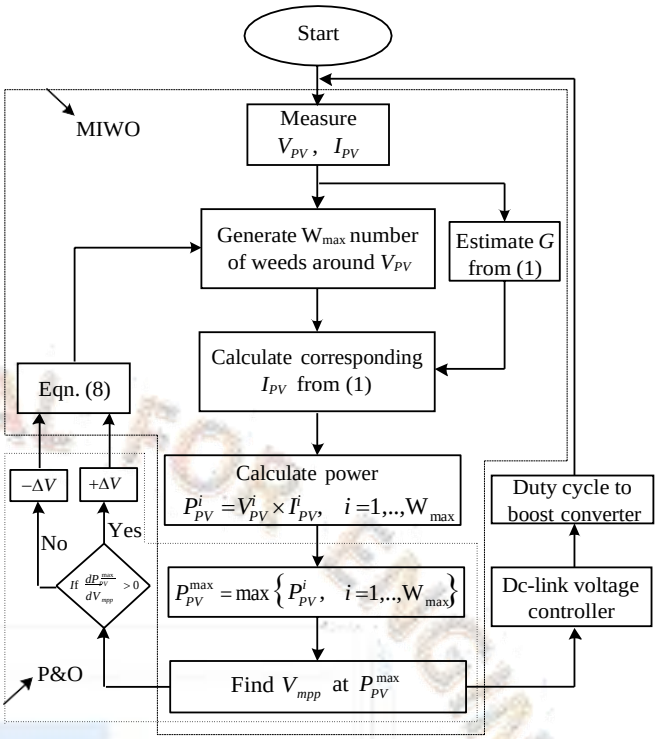

Fig. 7: Flowchart of the proposed system

IV. Simulation Results and Discussions

Simulation results are carried out with MATLAB/Simulink. The detailed parameters of PV system are mentioned in Appendix. The simulation results are discussed by considering the following case studies.

Case-1: *MPPT under change in irradiance*

Consider that irradiance changes from 1000W/m^2 to 800 W/m^2 at t=1 Sec. As shown in Fig. 8 (a). After a change in irradiance, proposed MPPT algorithm tracked properly V_{mpp} to get maximum power. The boost converter controller operates at V_{mpp}, hence, the system is operating at possible maximum power point. Corresponding V_{mpp} which is generated by the proposed MPPT algorithm as shown in Fig. 8(b). However, decreasing in irradiance can decrease the dc-link voltage in transient period (see Fig. 8 (c)). Hence, MPPT algorithm will increase the reference voltage momentarily which is shown in Fig. 8(b) after t=1 sec. After dc-link starts to increase, MPPT algorithm tries to reduce the reference voltage by voltage steeps as follows the Eqn. (8). This reference voltage is input to dc-link controller and boost converter controller regulates the V_{PV} at V_{mpp} as shown in Fig. 8 (c). Corresponding power is depicted in Fig. 8 (d). From Fig. 8 (d), it can be concluded that power generated by PV is following its reference signal.

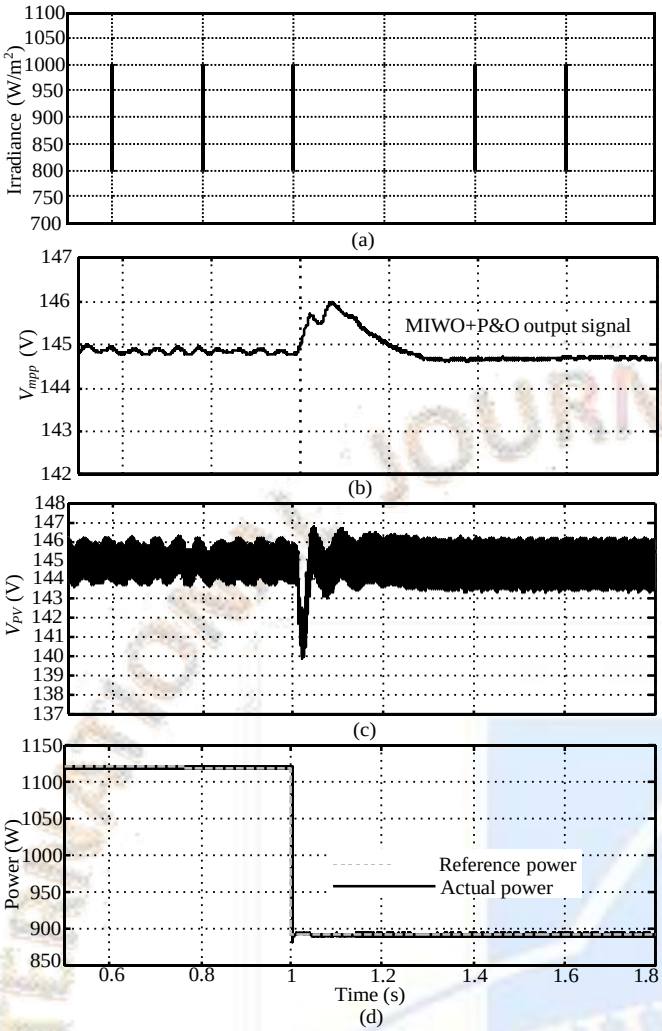

Fig. 8: (a) Change in irradiance, (b) Reference dc-link voltage (i.e., V_{mpp}), (c) V_{PV} (d) Reference and actual power generated by PV

Case-2: *MPPT under partial shading*

Generally PV array cannot receive uniform irradiance, under this situation; partial shading effect creates many local maximum power points. Proper V_{mpp} corresponding to global maximum proposing achieved by proposed MIWO based MPPT algorithm. Hence, the system can operate at maximum power point under partial shading condition. The conventional P&O algorithm can extract voltage corresponding to a first local minimum (which is near to present voltage point). Hence, integration of P&O with MIWO algorithm can work better and extract more power from the PV system in all the possible cases.

Now considered partial shading occurs at t=2.5 sec. Corresponding PV power is shown in Fig. 9. From Fig. 9, it can be concluded that, power generated from PV system is following possible maximum power from the PV system under partial shading condition. Hence, proposed controller can able to extract maximum power from a PV system.

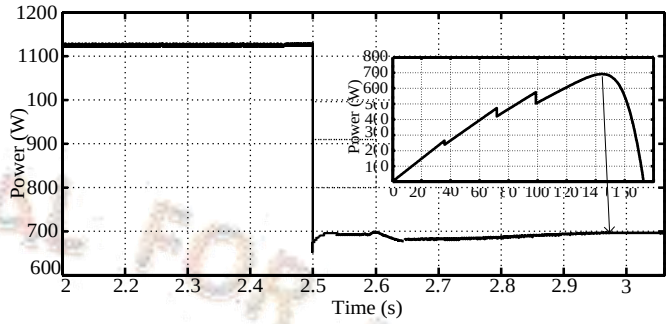

Fig. 9: PV power under partial shading

V. SMALL SIGNAL ANALYSIS

Non-linear model of the proposed system is obtained by nonlinear equations of the system blocks and corresponding non-linear block diagram of the proposed system (Fig. 1) is shown in Fig. 10. The system has non-linear relations, hence in order to analyze with small signal analysis, one has to convert the system to a linear system. The linearization of the nonlinear model of Fig. 10 is carried out using the small signal method.

The PV system linearized equation is obtained by (1) & (2) with the small signal method. A linear time-invariant model for the inductor current to the duty cycle of the boost converter is taken from [31]. The transfer function of inductor current to the duty cycle of the boost converter is followed by Eqn. (9) .

$$\frac{I_L(s)}{D(s)} = \frac{a_1(s+a_2)}{s^2 + a_3 s + a_4} \tag{9}$$

where,

$$a_1 = \frac{V_{PV}}{DL}, \quad D' = 1 - D, \quad a_2 = \frac{1}{C(R_L + R_C)}\left[1 + \frac{R_L D'}{R_C D' + R_L}\right],$$

$$a_3 = \frac{L + R_L R_C C D'}{(R_L + R_C)LC}, \quad a_4 = \frac{R_L D'(R_L D' + R_C)}{LC(R_L + R_C)^2}$$

The detailed linear model of the proposed system is shown in Fig. 14. However, linear model of MPPT is neglected and it is considered as one of the input signal to the dc-link controller due to its non-linear characteristics (i.e., its having sign function).

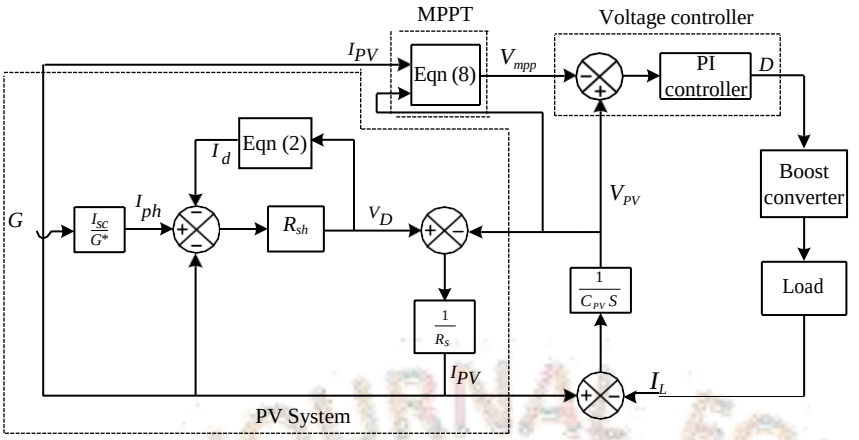

Fig. 10: Non-linear model

where $V_D = V_{PV} + I_{PV} R_s$

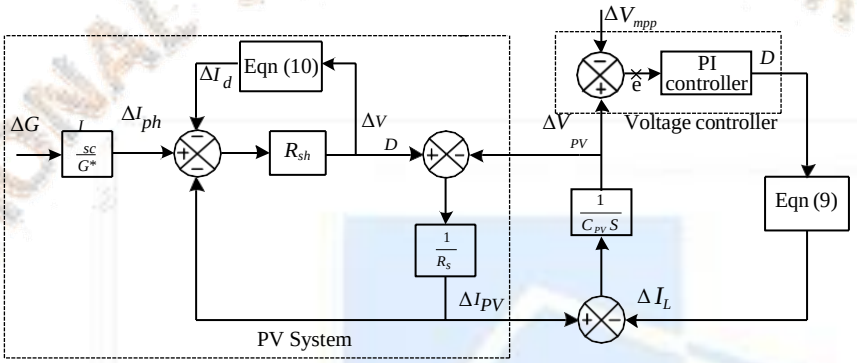

Fig. 141: Linearized model

$$\frac{I_{rs}}{V_t}\exp\left(\frac{V_D}{V_t}\right) \quad (10)$$

where $V_t = \frac{AKTn_s}{q}$

Transfer function of the Fig. 11 can be obtained by using block diagram reduction methods [35], as shown below

$$\frac{\Delta V_{dc}}{\Delta G} = \frac{a_5(s^3 + a_3 s^2 + a_4 s)}{b_3 s^4 + b_4 s^3 + b_5 s^2 + b_6 s + b_7} \quad (11)$$

$$\frac{\Delta V_{dc}}{\Delta V_{mpp}} = \frac{d\left(f_1 s^2 + f_2 s + f_3\right)}{b_3 s^4 + b_4 s^3 + b_5 s^2 + b_6 s + b_7} \quad (12)$$

where, $a_5 = b_{12}\left(\frac{I_{sc}}{G^*}\right)$, $b_3 = \frac{R_{sh}V_t}{V_t + R_{sh} I_{rs} e^{\left(\frac{V_D}{V_t}\right)}}$, $b_4 = \frac{1}{R_s}$,

$b_3 = C_{PV}\left(1 + b_1 b_2\right)$, $b_4 = C_{PV} a_3 \left(1 + b_1 b_2\right) + b_2$,

$b_5 = C_{PV} a_4 \left(1 + b_1 b_2\right) + a_3 b_2 + a_1 K_p \left(1 + b_1 b_2\right)$,

$b_6 = b_2 a_4 + \left(a_1 K_i + a_1 a_2 K_p\right)\left(1 + b_1 b_2\right)$,

$b_7 = a_1 a_2 K_i \left(1 + b_1 b_2\right)$, $d = a_1\left(1 + b_1 b_2\right)$,

$f_1 = K_p$, $f_2 = K_p a_2 + K_i$, $f_3 = a_2 K_i$

From (11) and (12), final transfer function can be written as

$$\Delta V_{PV} = \frac{a_5(s^3 + a_3 s^2 + a_4 s)\Delta G + d\left(f_1 s^2 + f_2 s + f_3\right)\Delta V_{mpp}}{b_3 s^4 + b_4 s^3 + b_5 s^2 + b_6 s + b_7} \quad (13)$$

The response of ΔV_{PV} corresponding to ΔG and ΔV_{mpp} can be obtained by Eqn. (13). Let us consider load resistance 40Ω and 10Ω. The response of **Error! Bookmark not defined.** with a 20% change in irradiance is depicted in Fig. 12. Consider that a 20% irradiance decreases at t=3 sec, and the 20% irradiance increases at t=3.3 sec. The corresponding responses of ΔV_{PV} with actual system (Fig. 1) and linearized system (i.e., Eqn. (13)) with aforementioned load resistances are shown in Fig. 12. From Fig. 15, it is shown that the responses are exactly overlapping as well as the response is better in case of low load resistance as shown in Fig. 12 (b). The load resistance can be adjusted by integrating energy storage such as a battery to system [36]. For better response, the battery can be connected at DC Bus through power electronics devices [37]. Hence, the DC Bus voltage can be regulated by maintaining at constant load current. The similar responses can obtained from Eqn. (13) for change in ΔV_{mpp}.

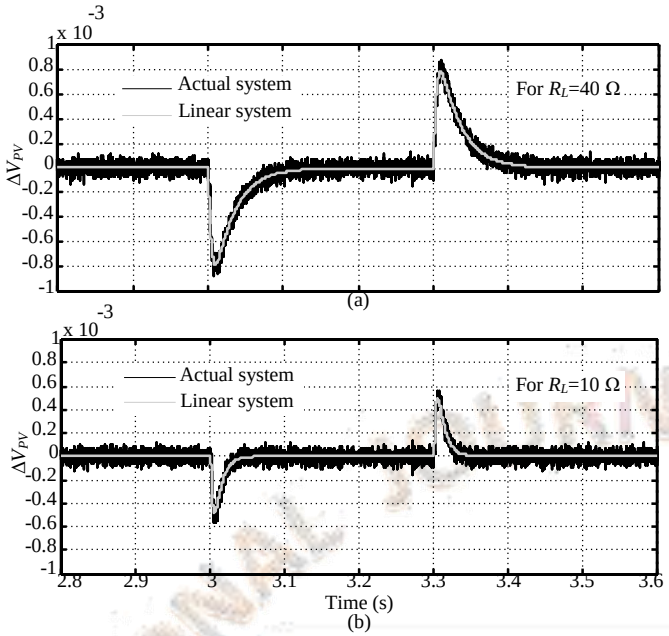

Fig. 15: PV base water pumping system without energy storage

As is well known, the loop robustness of a feedback system can characterize by gain margin (GM) and phase margin (PM). For a good design, one must have gain margin > 6 dB and phase margin > 30 deg [35]. For robustness study of the system of Fig. 14, loop transfer function is obtained when the loop is broken at 'e' (see Fig. 11). The loop transfer function (L_e) is shown in below:

$$L_e = \frac{-d\left(f_1 s^2 + f_2 s + f_3\right)}{g_1 s^4 + g_2 s^3 + g_3 s^2 + g_4 s} \quad (14)$$

where

$$g_1 = C_{PV}\left(1 + b_1 b_2\right),\ g_2 = C_{PV} a_3 \left(1 + b_1 b_2\right) + b_2,$$

$$g_3 = a_4 C_{PV}\left(1 + b_1 b_2\right) + a_3 b_2,\ g_4 = a_4 b_2$$

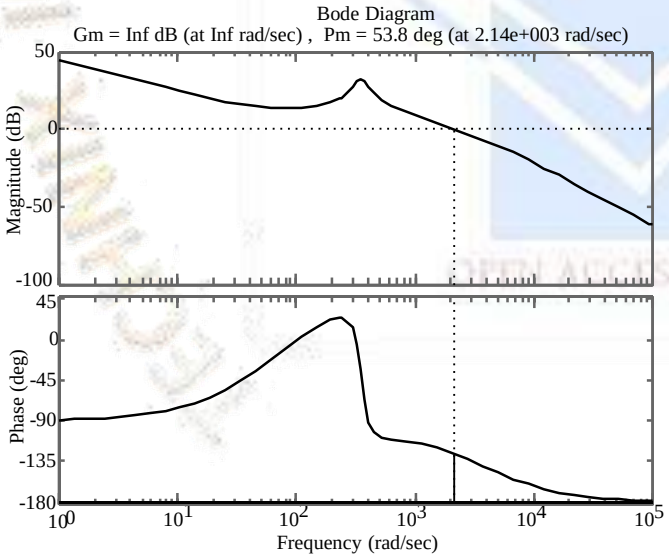

Fig. 16: The bode plot

The bode plots (indicating gain margin, phase margin, and gain crossover frequency) for the above loop transfer function (i.e. Eqn. (14)) is presented in Fig. 13 for R_L=40Ω. From Fig. 13, it can be concluded that the system is well robust.

VII. Conclussions

MIOW integrated with P&O algorithm based stand-alone PV based power generation system is presented in this paper. MIOW is integrated with a P&O algorithm for an effective operation of MPPT system under partially shaded PV system. Boost converter is considered for MPPT converter to extract the maximum power from PV. Using boost converter control, the power balance between PV and load is achieved by varying duty cycle. The PV system is operating at maximum power level in both normal as well as partial shading condition by regulating (V_{PV}) corresponding to V_{mmp} (generated by MPPT algorithm) with the boost converter controller. In this paper, battery is not considered, however, the response of the system can increase by adding a battery to the system. Small signal analysis is also done to show the strength to theory. The Different cases are discussed based upon changes in solar irradiance and partial shading condition. Loop robustness is presented with the help of a Bode plot of the loop transfer function. Through the MATLAB based simulation results in OPAL-RT platform, it is concluded that the performance of the controllers is satisfactory under conditions of changes in irradiance as well as under partial shading.

Appendix

Parameters of PV module

Simulation [38]	
Module Type	TP280
Maximum power (P_{pvmax})	280 W
Open circuit voltage (V_{oc})	44 V
Short circuit current (I_{sc})	8.28 A
Voltage at P_{pvmax} (V_{mpp})	36.2 V
Current at P_{pvmax} (I_{mpp})	7.73 A
Series resistance (R_s)/cell	0.0040 Ω
Parallel resistance (R_p)/cell	4.106 Ω
Module efficiency	14.1
Power tolerance	[-0 & +5]
Number of modules connected in series (N)	4

Parameters of boost converter

Simulation & Experiment	
Capacitance (C & C_{PV})	1000μF
Inductor (L)	1.3mH
Resistance (R_C)	0.15 Ω
Duty cycle (D)	0.6

Parameters of PI

Proportional gain (K_p)	0.03
Integral gain (K_i)	5.08

Parameters of P&O and MIWO

Step change in voltage (ΔV)	0.05
Maximum number of seeds (W_{max})	7

Parameters used in small signal model

For R_L	10 Ω	40 Ω
a_1	2.7846×10^5	2.7846×10^5
a_2	193.4833	49.5819
a_3	143.9939	70.8880
a_4	1.2395×10^5	1.233×10^5
a_5	8.6032×10^{-5}	8.6032×10^{-5}
b_1	0.003	0.003
b_2	3.4316	3.4316
b_3	0.0010	0.0010
b_4	3.5771	3.5033
b_5	9.0600×10^3	8.8085×10^3

b_6	34.877×10^5	22.709×10^5
b_7	2765.40×10^5	708.670×10^5
d	2.8135×10^5	2.8135×10^5
f_1	0.03	0.03
f_2	10.8845	6.5675
f_3	982.8951	251.8759
g_1	0.0010	0.00101
g_2	3.5771	3.5033
g_3	619.3674	367.8467
g_4	4.2534×10^5	4.2313×10^5

REFERENCES

[1] M. Liserre, T. Sauter and J. Y. Hung, "Renewable Energy Systems, Integrating Renewable Energy Sources into the Smart Power Grid through Industrial Electronics", *IEEE Industrial Electronics Magazine*, pp. 18-37, Mar. 2010.

[2] F. Blaabjerg, *et al*., ''Overview of control and grid synchronization for distributed power systems,'' *IEEE Transactions on Industrial Electronics*, Vol. 53, No. 5, pp. 1398–1409, Oct. 2006.

[3] J.-S. Lai, ''Power conditioning circuit topologies,'' *IEEE Industrial Electronics Magazine*., Vol. 3, No. 2, pp. 24–34, June 2009.

[4] G. Petrone, *et al*., ''Reliability issues in photovoltaic power processing systems,'' *IEEE Transactions on Industrial Electronics*, Vol. 55, No. 7, pp. 2569–2580, July 2008.

[5] J. H. R. Enslin, *et al*., "Integrated photovoltaic maximum power point tracking converter," *IEEE Transactions on Industrial Electronics.*, Vol. 44, No.6, pp. 769–773, Dec. 1997.

[6] Y-C Kuo, T-J. Liang and J-F. Chen, "Novel Maximum-Power-Point-Tracking Controller for Photovoltaic Energy Conversion System", *IEEE Transactions on Industrial Electronics*, Vol. 48, No. 3, pp. 594-601, June 2001.

[7] L. Bangyin, D. Shanxu and C. Tao, "Photovoltaic DC-building-module based BIPV system-concept and design considerations," *IEEE Transaction on Power Electronics*, Vol. 26, No. 5, pp. 1418–1429, May 2011.

[8] Z. Li, *et al*., "A modular grid connected photovoltaic generation system based onDC bus," *IEEE Transaction on Power Electronics*, Vol. 26, No. 2, pp. 523–531, Feb. 2011.

[9] J. L. Agorreta, *et al*., "Modeling and control of *N*-paralleled grid-connected inverters with LCL filter coupled due to grid impedance in PV plants," *IEEE Transaction on Power Electronics*, Vol. 26, No. 3, pp. 770–785, Mar. 2011.

[10] J. Y-Hyok, *et al*., "A real maximum power point tracking method for mismatching compensation in PV array under partially shaded conditions," *IEEE Transaction on Power Electronics*, Vol. 26, No. 4, pp. 1001–1009, Apr. 2011.

[11] Y. Bo, *et al*., "Design and analysis of a grid connected photovoltaic power system," *IEEE Transaction on Power Electronics*, Vol. 25, No. 4, pp. 992–1000, Apr. 2010.

[12] E. Serban and H. Serban, "A control strategy for a distributed power generation microgrid application with voltage- and current-controlled source converter," *IEEE Transaction on Power Electronics*, Vol. 25, No. 12, pp. 2981–2992, Dec. 2010.

[13] K. Ishaque, *et al*., "An Improved Particle Swarm Optimization (PSO)–Based MPPT for PV With Reduced Steady-State Oscillation", *IEEE Transaction on Power Electronics*, Vol. 27, No. 8, pp. 3627-3638. Aug. 2012

[14] B. I. Rani, G. S. Ilango and C. Nagamani, "Control Strategy for Power Flow Management in a PV System Supplying DC Loads", *IEEE Transactions on Industrial Electronics*, Vol. 60, No. 8, pp. 3185-3194, Aug. 2013.

[15] M. Amirabadi, *et al*., "High-Frequency AC-Link PV Inverter", *IEEE Transactions on Industrial Electronics*, Vol. 61, No. 1, pp. 281-291, Jan. 2014.

[16] C. N. Bhende and S. G. Malla, "Novel Control of Photovoltaic based Water Pumping System without Energy Storage", *International Journal of Emerging Electric Power Systems*, Vol. 13, No. 5, Nov. 2012.

[17] Y-C. Kuo, T-J. Liang and J-F. Chen, "Novel Maximum-Power-Point-Tracking Controller for Photovoltaic Energy Conversion System", *IEEE Transactions on Industrial Electronics*, Vol. 48, No. 3, pp. 594-601, June 2001.

[18] R. Gules, *et al*, "A Maximum Power Point Tracking System With Parallel Connection for PV Stand-Alone Applications", *IEEE Transactions on Industrial Electronics*, Vol. 55, No. 7, pp. 2674-2683, Jul. 2008.

[19] H. Patel and V. Agarwal, "Maximum Power Point Tracking Scheme for PV Systems Operating Under Partially Shaded Conditions", *IEEE Transactions on Industrial Electronics*, Vol. 55, No. 4, pp. 1689-1698, Apr. 2008.

[20] Emilio Mamarelis, Giovanni Petrone and Giovanni Spagnuolo, "Design of a Sliding-Mode-Controlled SEPIC for PV MPPT Applications", *IEEE Transactions on Industrial electronics*, Vol. 61, No. 7, pp. 3387-3398, Jul. 2014.

[21] G. Petrone, Giovanni Spagnuolo and Massimo Vitelli, "An Analog Technique for Distributed MPPT PV Applications", *IEEE Transactions on Industrial Electronics*, Vol. 59, No. 12, pp. 4713-4722, Dec. 2012.

[22] H. Patel, Vivek A., "MATLAB-Based Modeling to Study the Effects of Partial Shading on PV Array Characteristics", *IEEE Transactions on Energy Conversion*, Vol. 23, No. 1, pp. 302-310, Mar. 2008.

[23] L. Gao, *et al,* "Parallel-Connected Solar PV System to Address Partial and Rapidly Fluctuating Shadow Conditions", *IEEE Transactions on Industrial Electronics*, Vol. 56, No. 5, pp. 1548-1556, May 2009.

[24] L. F. L. Villa, *et al*., "A Power Electronics Equalizer Application for Partially Shaded Photovoltaic Modules", *IEEE Transactions on Industrial Electronics*, Vol. 60, No. 3, pp. 1179-1190, Mar. 2013.

[25] R. Toscano and P. Lyonnet, "A Kalman Optimization Approach for Solving Some Industrial Electronics Problems", *IEEE Transactions on Industrial Electronics*, Vol. 59, No. 11, pp. 4456-4464, Nov. 2012.

[26] Sun Yuantao and Zhang Qing, "Based on the Cauchy Distribution Reproduce Mode Improved IWO Algorithm Research and Application", *2nd International Conference on Information Science and Engineering (ICISE)*, Hangzhou, China, pp. 1057-1060, 4-6 Dec. 2010.

[27] S. Karimkashi and A. A. Kishk, "Invasive Weed Optimization and its Features in Electromagnetics", *IEEE Transaction on Antennas and Propagation*, Vol. 58, No. 4, pp. 1269-1278, Apr. 2010.

[28] Eduardo Román, *et al*, "Intelligent PV Module for Grid-Connected PV Systems", *IEEE Transactions on Industrial Electronics*, Vol. 53, No. 4, pp. 1066-1073, Aug. 2006.

[29] A. R. Mehrabian and C. Lucas, "A Novel Numerical Optimization Algorithm Inspired from Weed Colonization", *Ecological Informatics*, Vol. 1, Issue 4, pp. 355-366, Dec. 2006.

[30] X. Yao, Y. Liu and G. Lin, "Evolutionary Programming Made Faster", *IEEE Transactions on Evolutionary Computation*, Vol. 3, No. 2, pp. 82-102, July 1999.

[31] B. Johansson, "Improved Models for DC-DC Converters", *Licentiate Thesis*, Department of Industrial Electrical Engineering and Automation, Lund University, Lund, 2003.

[32] Y. Li, *et al*., "Current Mode Control for Boost Converters With Constant Power Loads", *IEEE Transactions on Circuits and Systems-I*: Regular papers, Vol. 59, No. 1, pp. 198-206, Jan. 2012.

[33] C. N. Bhende, S. Mishra and S. K. Jain, "TS-fuzzy-controlled active power filter for load compensation", *IEEE Transactions on Power Delivery*, Vol. 21, No. 3, pp. 1459-1465, July 2006.

[34] A. M. Noman, K. E. Addoweesh and H. M. Mashaly, "DSPACE Real-Time Implementation of MPPT-Based FLC Method", *International Journal of Photoenergy*, Hindawi Publishing Corporation, Vol. 2013, Article ID 549273, 11 pages.

[35] R. C. Dorf, and R. H. Bishop, "Modern Control Systems", Pearson Education, Inc, 2008.

[36] H. Beltran, *et al*., "Evaluation of Storage Energy Requirements for Constant Production in PV Power Plants", *IEEE Transactions on Industrial Electronics*, Vol. 60, No. 3, pp. 1225-1234, Mar. 2013.

[37] B. K. Bose, "Global Energy Scenario and Impact of Power Electronics in 21st Century", *IEEE Transactions on Industrial Electronics*, Vol. 60, No. 7, pp. 2638-2651, July 2013.

[38] http://www.4-dgroup.com/4d/PDF/Tata%20300.pdf